Table 1 Definition of intensity of turbulence

Frequently occurring peak g increment	Descriptive term
±0.05–±0.10	very light
±0.10–±0.25	light
±0.25–±0.50	moderate
±0.50–±0.75	severe
±0.75 or greater	extreme

It is obvious from the definitions given in the previous paragraph that the subjective element in the selection of turbulence samples was not negligible. Subjective judgment was used to determine, for example, if the oscillogram traces indicated one long turbulent region or two or more closely spaced turbulent regions. Throughout the HICAT program more than one person edited the oscillogram records. Even though a strong effort was made to obtain uniformity in judgment, individual differences in judgment probably were not eliminated. In addition, changes in judgment on the length of a run undoubtedly occurred as individual experience was gained. A relatively high number of samples at the even 4, 6, 7, and 10 min indicates some personal bias. An arbitrary upper limit of 1000 sec was established because of the data processing computer program. Thus, the statistical information presented in Fig. 1 is biased because of the elimination of the very short and the very long turbulent regions; because the pilot, in a few cases, turned the aircraft before completely penetrating the turbulent regions and because the criteria for the intensity of turbulence do not include the gust velocities. On the whole, however, the results presented in Fig. 1 probably provide an adequate representation of the relative frequencies of occurrence of the turbulent regions whose length are in the intermediate range.

Further measurements and analysis are required to answer relevant questions such as 1) What are the horizontal shapes of the turbulent regions? 2) How do the shapes and lengths change in time with respect to axis fixed to the earth and with respect to axis fixed to a volume element of the atmosphere?

References

[1] Crooks, W. M. et al., "Project HICAT An Investigation of High Altitude Clear Air Turbulence," TR AFFDL-TR-67-123, Nov. 1967, Lockheed-California Co., Burbank, Calif.

[2] Crooks, W. M. et al., "Project HICAT High Altitude Lear Air Turbulence Measurements and Meteorological Correlations," TR AFFDL-TR-68-127, Nov. 1968, Lockheed-California Co., Burbank, Calif.

An Algorithm for the Induced Velocity of Curved Vortex Lines

THOMAS ARTHUR MCMAHON*
Massachusetts Institute of Technology, Cambridge, Mass.

Nomenclature

Ψ = stream function
Γ = circulation about vortex ring, vortex line
V_z = normal component of induced velocity
R = vortex ring radius
r,z = field point coordinates (dimensional)
θ_i,θ_r = angles of incidence and reflection of hypothetical rays
x = dimensionless radial distance, r/R
∂ = dimensionless axial distance, z/R

Received February 28, 1969.
* Research Assistant.

Introduction

MANY problems in aerodynamics, such as propeller theory and rotary wind theory, involve calculating the induced velocity due to curved vortex lines. Provided one knows the geometry of such lines, the induced velocity at any point may be calculated by the Biot-Savart law. Occasionally it is useful to have a scheme for approximating the line integration this law requires. Such a scheme is advanced here.

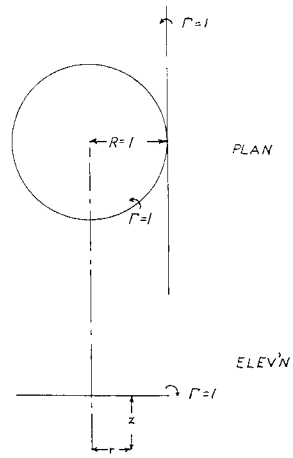

Fig. 1 Coordinate system

Proposing the Algorithm

Consider the geometry of Fig. 1, which represents a vortex ring and a tangent vortex line of equal strength. It is proposed to calculate the normal component of induced velocity due to the ring in any plane parallel to the plane of the ring and displaced a height z, and to compare it with that appropriate for the vortex line. The stream function at a point P in the flowfield of a vortex ring of strength Γ and radius R is given in Ref. 2 as

$$\Psi = -(\Gamma R/2)(d_1 + d_2)[K(\tau) - E(\tau)] \qquad (1)$$

where Rd_1 and Rd_2 are the least and greatest distances of the point P to the vortex ring,

$$\tau = (d_2 - d_1)/(d_2 + d_1) \qquad (2)$$

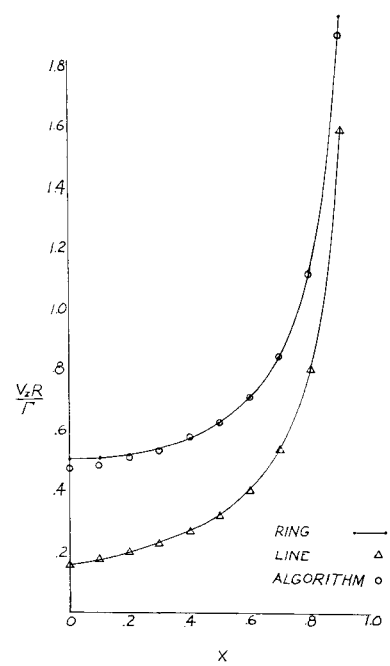

Fig. 2. Induced velocity comparison, $\partial = z/R = 0$.

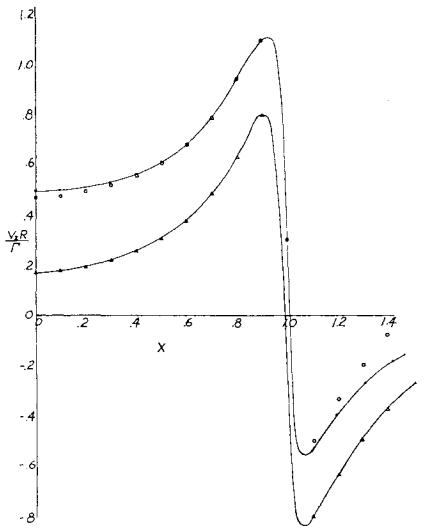

a) $\delta = 0.1$

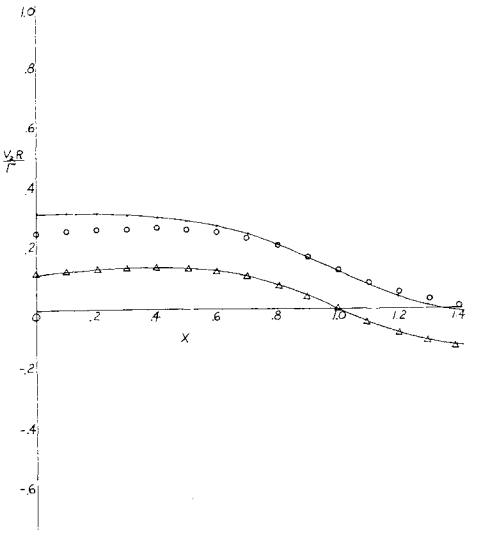

d) $\delta = 0.6$

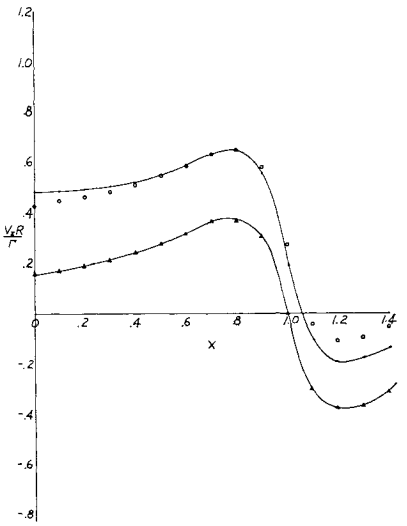

b) $\delta = 0.2$

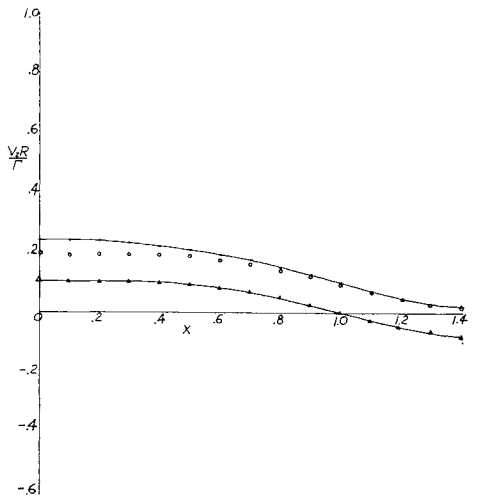

e) $\delta = 0.8$

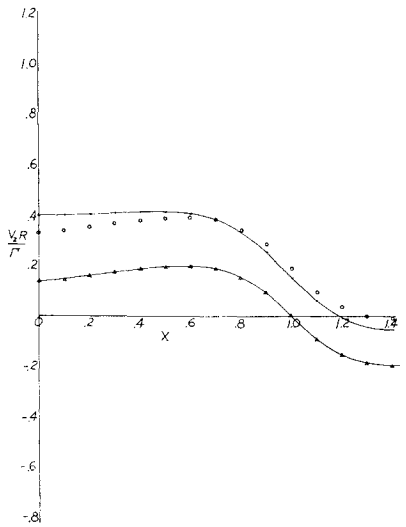

c) $\delta = 0.4$

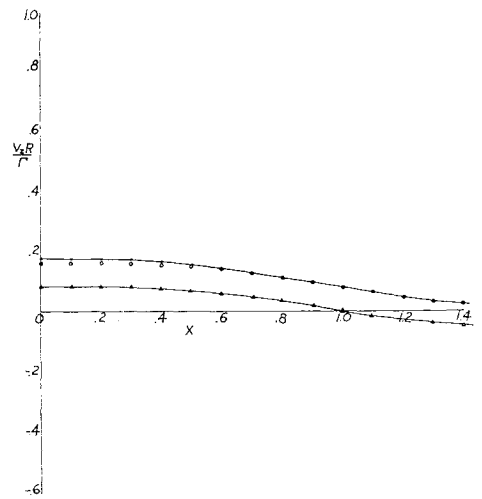

f) $\delta = 1.0$

Fig. 3 Induced velocity comparison.

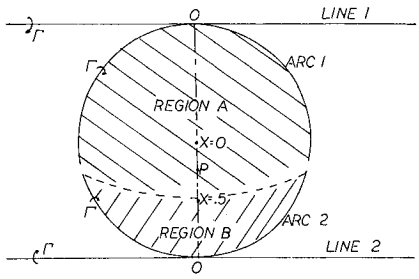

Fig. 4a The ring is divided into two arcs.

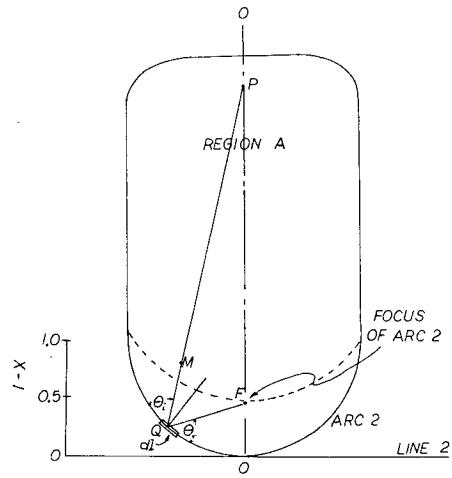

Fig. 4b Evaluating k.

and $K(\tau)$ and $E(\tau)$ are the complete elliptic integrals of the first and second kinds, respectively. A table appears in Ref. 1 of the normal component of induced velocity in the vicinity of a vortex ring calculated from (1). Figures 2 and 3 are plotted using data from this table.

Figure 2 shows the preceding comparison when $\delta = 0$, i.e., when the field point and the ring plus its tangent line are in the same plane. One sees that the velocity due to the line fails to approximate that due to the ring, falling short by nearly 100% over most of the nondimensional radial distance, but that the numerical value by which the line falls short of the ring is nearly equal to that line-induced normal velocity V_z evaluated at a distance from the line of $x = r/R = 0.5$. In fact, if the number $V_z(0.5)$ is added as a constant to every point of the velocity plot due to the line, a remarkable coincidence with the plot due to the ring occurs, as may be seen in Fig. 2. We therefore propose that an algorithm for approximating the normal induced velocity due to a vortex ring shall be

$$V_z = \frac{(1-x)}{2\pi[(1-x)^2+\delta^2]} + \frac{(0.5)}{2\pi[(0.5)^2+\delta^2]} \qquad (3)$$

Graphical Tests of the Algorithm

Figures 3a–3f show the induced velocity due to a vortex ring, as tabulated in Ref. 1, plotted for various normalized displacement heights z/R of the field point plane. In each plot, the algorithm is able to bring the ring and line data nearly into coincidence over some major part of the dimensionless radial distance scale. It is apparent that the region of best coincidence moves to slightly larger dimensionless radii as the height of the field point plane increases.

A Geometric Argument

Having made the observation that the algorithm (3) seems to work, the question becomes, Why does it work? We present a short argument demonstrating that, if one is willing to start with two qualitative postulates about the induction properties of vortex semicircular arcs and lines, the quantitative constant contained in one of the postulates may be evaluated, demonstrating how the algorithm is an approximative integration of the Biot-Savart law. In Fig. 4a, we consider the case when $z = 0$, i.e., the field point and the ring are coplanar. The ring is divided into two arcs, one lying above the field point P and the other below. The area included by the circle is divided into two regions.

First Postulate: The normal component of induced velocity due to vortex arc 2 on the line 0-0 in region B is equal to that due to an imaginary line, line 2.

Second Postulate: The induced velocity due to arc 1 in region B is equal, on a line 0-0, to a constant k. In Fig. 4b the region A of constancy of induced velocity is exaggerated to demonstrate that region A is relatively far from arc 2.

The increment added to the induced velocity at point M in region A due to a small rotational element dl is identical to that added to point P or any other point in region A (by the second postulate). When the summing of the induced velocity due to each element dl is completed, we see that the induced velocity at P is identical with that at F. Then, by postulate 1, we replace arc 2 by line 2, and compute the induced velocity at F due to line 2. It is evident that the constant k in the second postulate is approximately equal to the induced velocity due to the line at nondimensional distance 0.5, just as we observed graphically in formulating the algorithm. One may see that the foregoing geometric syllogism is valid also when one considers field points in planes when $z \neq 0$, because then the angles θ_i and θ_r are still equal, and the lengths QM and QF of rays from dl are now projections of other, also equal, three-dimensional rays. We return to the earlier observation that the region of best coincidence between vortex ring data and the proposed algorithm moves to greater radii as the height of the field point increases: this is interpreted as a property of the first postulate, which fails when $x = r/R > 1$ if z is small, but becomes more successful at the larger radii for moderate values of z.

Conclusions

An implication of the geometric syllogism is that the far field of any truncated curved arc is nearly a constant, and this constant may be evaluated once the approximate focus of the arc is known. This means that the induction field due to vortex patterns with complicated plan projections might be profitably calculated by considering large curved vortex segments, rather than shorter straight ones.

A further use of the proposed algorithm might arise in calculations of the magnetic field due to curved, current-carrying conductors. In the special case of currents around a body of revolution, the algorithm is able to reduce a three-dimensional calculation to one involving only two dimensions. Here, employing the algorithm would be equivalent to performing an integration over the azimuth variable.

References

[1] Castles, W. and De Leeuw, J. H., "The Normal Component of the Induced Velocity of a Lifting Rotor and Some Examples of Its Application," Rept. 1184, 1954, NACA.

[2] Lamb, H., *Hydrodynamics*, 6th ed., Dover, New York, 1945.